

1 **UAS and a virtual environment as possible response tools to the incidents**  
2 **involving uncontrolled release of dangerous gases – a case study**

3  
4 Anna Rabajczyk<sup>1\*</sup>, Jacek Zboina<sup>1</sup>, Maria Zielecka<sup>1</sup>, Radosław Fellner<sup>2</sup>, Piotr Kaczmarzyk<sup>1</sup>,  
5 Dariusz Pietrzela<sup>1</sup> and Grzegorz Zawistowski<sup>1</sup>

6  
7 <sup>1</sup> Scientific and Research Centre for Fire Protection, National Research Institute, Nadwiślańska  
8 213, 05-420 Józefów, Poland; [arabajczyk@cnbop.pl](mailto:arabajczyk@cnbop.pl) (A.R.); [jzboina@cnbop.pl](mailto:jzboina@cnbop.pl) (J.Z.);  
9 [mzielecka@cnbop.pl](mailto:mzielecka@cnbop.pl) (M.Z.); [pkaczmarzyk@cnbop.pl](mailto:pkaczmarzyk@cnbop.pl) (P.K.); [dpietrzela@cnbop.pl](mailto:dpietrzela@cnbop.pl) (D.P.);  
10 [gzawistowski@cnbop.pl](mailto:gzawistowski@cnbop.pl) (G.Z.)

11 <sup>2</sup> Fire University of Warsaw, Słowackiego 52/54, 01-629 Warsaw, Poland;  
12 [rfellner@apoz.edu.pl](mailto:rfellner@apoz.edu.pl) (R.F.)

13 \* Correspondence: [arabajczyk@cnbop.pl](mailto:arabajczyk@cnbop.pl); Tel.: +48-22-769-32-69, Fax: +48-22-769-33-73  
14 (A.R.)

15  
16 **Abstract:** Various types of events and emergency situations have a significant impact on the  
17 safety of people and the environment. This especially refers to the incidents involving the  
18 emission of pollutants, such as ammonia, into the atmosphere. The article presents the concept  
19 of combining unmanned aerial vehicles with contamination plume modelling. Such a solution  
20 allows for mapping negative effects of ammonia release caused by the damage to a tank (with  
21 set parameters) during its transport as well as by the point leakage (such as unsealing in the  
22 installation). Simulation based on the ALOHA model makes it possible to indicate the direction  
23 of pollution spread and constitutes the basis for taking action. And, the use of a drone allows to  
24 control contamination in real time and verify the probability of a threat occurring in a given  
25 area.

26 **Keywords:** unmanned aerial system (UAS); ammonia; emergency situations; ALOHA

27

28

This article has been accepted for publication and undergone full peer review but has not been through the copyediting, typesetting, pagination and proofreading process which may lead to differences between this version and the version of record. Please cite this article as DOI: [10.24425/cpe.2024.149460](https://doi.org/10.24425/cpe.2024.149460).

Received: 11 December 2023 | Revised: 13 February 2024 | Accepted: 29 February 2024



## 29 1. Introduction

30 In various sources migration of natural and anthropogenic substances is more and more often  
31 presented in the form of mathematical models. These, in turn, are assumed to reflect the real  
32 world. These models enable the prediction of a chemical's concentration in different  
33 environmental components and at various times, provided that the amount of the chemical  
34 released into the environment, i.e. the pollutant's load, is known. (Bessagnet et al., 2020). The  
35 behaviour and spread of a chemical in the environment depends on its physicochemical  
36 properties, the way it is introduced into the environment, and the characteristics of the  
37 environment into which it is released (National Academies of Sciences, Engineering, and  
38 Medicine, 2016). Models are used to integrate information on the multiple processes of  
39 transport and chemical transformations. They make it possible to present the behaviour and  
40 migration of a chemical compound in the environment in an accessible and transparent manner  
41 (Rasheed et al., 2019; Batstone et al., 2015; Pirrone et al., 2010; Al Fayed et al., 2019; Giompapa  
42 et al., 2007).

43 One of such substances is ammonia, which clearly affects air quality, contribute to  
44 environmental and climate changes, as well as, poses a threat to human life and health (Van  
45 Damme et al., 2018; Zheng et al., 2015). Ammonia was included as a significant air pollutant  
46 in the Gothenburg Protocol of 1999 (UNECE, 1999) with later annexes (UNECE, 2019). It  
47 plays a key role in the nitrogen cycle and is the main component of the total reactive nitrogen  
48 present in the atmosphere. It should be remembered that the harmful effects of ammonia on  
49 humans is mainly due to the deterioration of pulmonary function and visual disturbances (Bai  
50 et al., 2006; Bittman et al., 2015; Naseem and King, 2018). Ammonia is quickly absorbed and  
51 excreted in the upper respiratory tract, therefore, it does not cause changes in the deeper tissues  
52 of the body (Malm et al., 2013). There is no information on the teratogenic, genotoxic or  
53 carcinogenic effects of ammonia in the available literature. However, exposure to  
54 concentrations above 2,500 ppm can be fatal if the duration of exposure exceeds 30 minutes  
55 and is immediately lethal at 5,000 ppm (Neghab et al., 2018). Consequently, an increase in NH<sub>3</sub>  
56 emissions has a negative impact on the environment and public health, and may also affect  
57 climate change (Giannakis et al., 2019). For these reasons, it is vital to take appropriate action  
58 in the event of a risk of uncontrolled emission of this gas to the environment and to minimize  
59 the risk to entities involved in response to such a threat.

60 The available data show that the largest source of NH<sub>3</sub> emissions, accounting for over 95% of  
61 its emissions, is agriculture, including livestock farming and the use of NH<sub>3</sub>-based fertilizers  
62 (Battye et al., 2003; Fu et al., 2020; Pan et al., 2022; Wyer et al., 2022). Other sources of NH<sub>3</sub>

63 include industrial processes, vehicle emissions and volatilization from soils and oceans (Sapek,  
64 2013; Sutton et al., 2000; Wu et al., 2020; Wu et al., 2016; Zhan et al., 2021). Recent studies  
65 indicate that  $\text{NH}_3$  emissions increased by 90% on a global scale over the last few decades, i.e.,  
66 from 1970 to 2005 (Sommer et al., 2019). For the first decade of the 21st century, the EDGAR  
67 emissions model reports a 20% increase of the global  $\text{NH}_3$  emissions, but with large variations  
68 at regional and national scales (Van Damme et al., 2021; Luo et al., 2022; Liu et al., 2022). An  
69 additional difficulty is the fact that ammonia is often released in less populated or border areas,  
70 where ~~there are fewer buildings and~~ there is not a sufficient network of measuring stations.  
71 Constantly increasing air pollution makes it extremely important to control the quality of air.  
72 Monitoring systems are commonly used for this purpose, especially in urban areas and places  
73 of social and economic importance. In the case of regions with lower population density the  
74 distribution of elements in the permanent air quality monitoring systems is less common. This  
75 is due to economic reasons, i.e. the cost of purchase and operation of such systems. Available  
76 and constituting a large potential for air quality control and monitoring is an application of  
77 unmanned aerial vehicles (UAVs) with appropriate detectors and cameras, the choice of which  
78 depends on the purpose and scope of measurements as well as the monitored pollutant. Small  
79 unmanned aerial vehicles (mini-UAVs) equipped with specialized sensors for pollution analysis  
80 provide new approaches and research opportunities in the field of air quality monitoring and  
81 identification of emission sources. They also find applications in the atmosphere research by  
82 identifying, for example, trends in climate changes (Xiang et al., 2019) or directions of  
83 processes taking place in the atmosphere (Zappa et al., 2020) or in the case of crisis management  
84 (AIRBEAM, 2022; CAMELOT, 2023; COMPASS2020, 2023).

85 The use of UAV may be particularly important for the monitoring of gaseous pollutants  
86 leakages which sources are difficult to access and at the same time strategic for international or  
87 interregional cooperation. Such incidents may have serious consequences for the environment  
88 and the population due to the possibility of movement of the pollution cloud. Even worse, they  
89 can spread to the border areas or to the territory of a neighbouring region or state. Correctly  
90 applied protective measures require the best possible knowledge of the source of pollutant  
91 emission, trajectory of contamination movement and the negative impact on the biosphere,  
92 including humans. Therefore, when it is impossible to use stationary monitoring points, in  
93 places beyond the station's reach, it may be necessary to use autonomous platforms. The use of  
94 the atmospheric dispersion model showed that two UAVs are able to provide results of a quality  
95 comparable to a stationary monitoring network (Thyker-Nielsen et al., 1999; Hiemstra et al.,  
96 2011; Šmídl and Hofman, 2013).

97 Application of UAVs equipped with appropriate detectors and cameras is more commonly  
98 applied nowadays. UAVs use for detection of contamination, harmful gases presents new  
99 possibilities during operations and for procedures in the event of an incident and gas release  
100 (Rabajczyk et al., 2020; Jońca et al. 2022). For example, UAVs were used to detect gas leaks  
101 and damage to the thermal insulation of tanks at the Guiana Space Center (Ferlin et al., 2019),  
102 or during the gas explosion accident and a gas pipeline fire in Murowana Goślina (Gaz SYStem,  
103 2018), extinguishing forest fires and mitigating the damage caused by fires using early detection  
104 methods (Kinaneva et al., 2019), optimization of the rescue operation in the event of a fire at  
105 Notre Dame (Vidi, 2019), gas emissions in the event of volcanic eruptions (Everts and  
106 Davenport, 2016) or detection of ethanol, formaldehyde, ammonia, or hydrogen chloride in  
107 residential neighbourhoods (Pobkrut et al., 2016; Jaferník, 2019; Burgués and Marco, 2020).  
108 The article describes the use of an UAV equipped with an ammonia sensor as well as the  
109 ALOHA (Areal Locations of Hazardous Atmospheres) modelling program. The aim of this  
110 paper is to present the concept of combining unmanned aerial vehicles with contamination  
111 plume modelling on the example of ammonia emissions in a virtual environment. This approach  
112 has been developed within a scientific and development work carried out as a part of the project  
113 entitled "Controlling an autonomous drone using goggles (monocular)" for the needs of the  
114 Polish Border Guard.

115 In the first stage, simulations of the ammonia plume spread for two events were carried out.  
116 They aim was to determine the minimum information necessary for the proper management of  
117 the action with the use of drones and a virtual drone control system. Next, the results of  
118 simulations using the ALOHA program were implemented in scenarios of ammonia emissions  
119 from tank and from the point source formed due to unsealing created in the pipeline. Then, the  
120 results obtained were analysed in terms of the possibility of using them in the newly developed  
121 system: for selection of parameters and drone's construction (including: type of sensors, weight,  
122 design) and, in the end, assessment of the usefulness of this system in case of the absence of  
123 permanent monitoring points.

124

## 125 **2. Material and methods**

### 126 *2.1. Simulation requirements for the ALOHA program*

127 The computer program ALOHA (Areal Locations of Hazardous Atmospheres) was used to  
128 perform the simulation. In general, the functions included in the program can be used to model  
129 the following phenomena: release and dispersion (for low or heavy gases), influence of

130 averaged terrain roughness, liquid fire in the tank, pool fires, jet fire and explosion (The  
131 CAMEO® Software Suite, 2016).

132 To perform dispersion simulations, which are the subject of this study, the Gauss model was  
133 used. The formula of the Gauss model used in the ALOHA program is described by the equation  
134 (Bhattacharya and Kumar, 2015):

$$135 \quad C(x, y, z) = \frac{Q}{2\pi\sigma_y\sigma_z u} \exp\left(-\frac{1}{2}\left(\frac{y}{\sigma_y}\right)^2\right) \cdot \left(\exp\left(-\frac{1}{2}\left(\frac{z-H}{\sigma_z}\right)^2\right) + \exp\left(-\frac{1}{2}\left(\frac{z+H}{\sigma_z}\right)^2\right)\right) \quad (1)$$

136 where:

137  $C$  – pollutant concentration at a given point [ $\text{g}/\text{m}^3$ ],

138  $x, y, z$  – distance from source ( $x$  – downwind,  $y$  – crosswind,  $z$  – vertical)

139  $u$  – the average wind speed [ $\text{m}/\text{s}$ ],

140  $H$  – effective emission height (sum of emitter height and plume elevation) [ $\text{m}$ ],

141  $Q$  – pollutant emission rate,

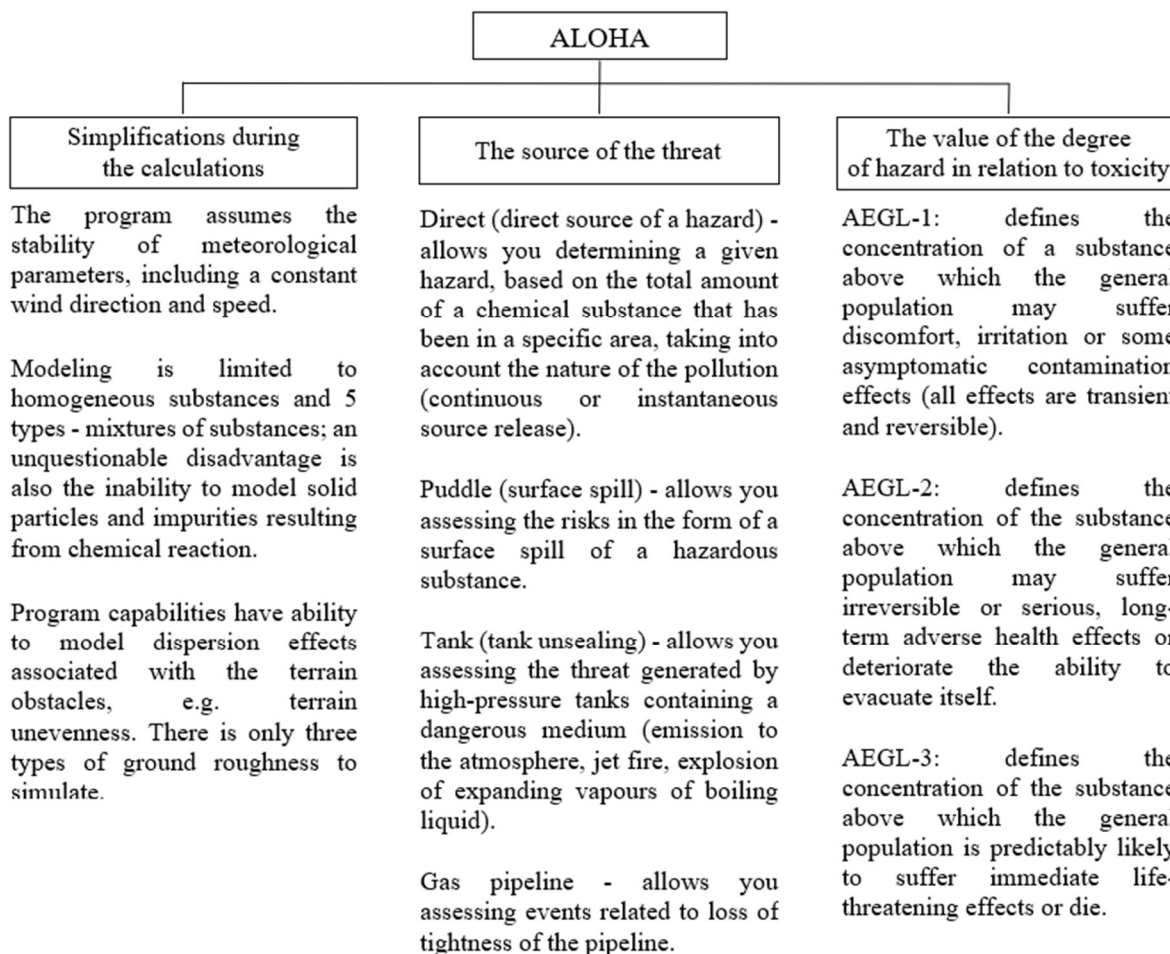
142  $\sigma_y, \sigma_z$  – standard deviations (dispersion parameters) determined as functions of vertical  
143 turbulence states and the distance of the receptor from the emission source, estimated on the  
144 basis of the atmospheric stability class (dispersion coefficients are calculated by the ALOHA  
145 program, based on given stability class, according to the algebraic expressions developed by  
146 Briggs G.A. (Hanna et al., 1982; U.S. Department of Energy, 2004; U.S. Department of Energy,  
147 2007).

148 Referring to simulation tool, it should be remembered that the program uses some  
149 simplifications during the calculations, including the lack of modelling the dispersion effects  
150 associated with the terrain obstacles, e.g., terrain unevenness (Fig. 1) (Lee et al., 2018).

151 ALOHA takes into account the indicated phenomena by dividing the transport equations into  
152 three emission zones with appropriately selected factors, such as the dispersion parameters. To  
153 create an appropriate emergency release scenario, the program's capabilities allow to  
154 characterize the source of the threat as direct, puddle, tank and gas pipeline (Fu et al., 2020;  
155 Brown Coal Innovation Australia Limited, 2015). The simulation based on the ALOHA  
156 program makes it possible to determine the time in which the substance will be released into  
157 the environment, the range of the impact of the event in the selected direction, and taking into  
158 account the prevailing meteorological conditions. It can also estimate the concentration of the  
159 chemical substance as a function of distance and time from the leak location.

160 In order to determine the value of the degree of hazard in relation to toxicity, the parameter  
161 AEGL (Acute Exposure Guideline Level) is used, defined as the toxicological threshold values  
162 of the concentration of a substance directly hazardous to humans (Fig. 1) (The CAMEO®

163 Software Suite, 2016; National Research Council, 2001; Acute Exposure Guideline Level,  
164 2016).



165

166 Figure 1. Characteristics of selected limitations and applications of the ALOHA program (Fu  
167 et al., 2020; Lee et al., 2018; Brown Coal Innovation Australia Limited, 2015; The CAMEO®  
168 Software Suite, 2016; National Research Council, 2001).

169

## 170 2.2. Modelling data – case study

171 The simulations included selected parameters reflecting real conditions, which allowed for  
172 presenting the risk of ammonia dispersion in the event of two representative situations, i.e., a  
173 tank with given characteristics (Table 1) and a leak point (Table 1) under specific conditions  
174 (Table 2). Cylindrical tanks are very often used in industrial plants and in transport. The point  
175 source simulates the emission conditions from the pipeline failure carrying the gas. The  
176 parameters (Table 2) used for the simulation correspond to the assumptions used to create  
177 emergency plans (documents developed in the event of an accident, unpredictable  
178 circumstances and sudden events and developed individually by the units responsible for

179 security) by the State Fire Service, equipped with specialized gear designed to fight fires,  
 180 natural disasters and other local threats. The simulation also takes into account criteria  
 181 important for the correct conduct of the action and allows to develop a strategy for using the  
 182 drone and controlling the drone based on a monocular.

183

184 Table 1. Parameters used to simulate ammonia emissions for the ALOHA / RAILCAR model  
 185 for all scenarios.

Parameter	Characteristic
Simulated phenomenon: Tank emission	
Medium	NH <sub>3</sub>
Leakage from tank	Diameter: 2.3 m Length: 13.4 m Volume: 55,674 dm <sup>3</sup> Filling of the tank with NH <sub>3</sub> : 50%
The roughness of the substrate	Open country
Cloudy	Partly cloudy
Inversion height [m]	Without inversion
Air humidity [%]	50
Internal tank temperature [°C]	Ambient temperature
Ammonia mass – resultant [kg]	17889
Description of the release	Hole, without ignition, emissions to the atmosphere
Hole	Round, diameter 0.1 m
Physical state	50% liquid
Simulated phenomenon: Direct source of a hazard	
Medium	NH <sub>3</sub>
Leakage from tank	50 kg/s, duration: 30 min
The roughness of the substrate	Open country
Cloudy	Partly cloudy
Inversion height [m]	Without inversion
Air humidity [%]	50
Internal tank temperature [°C]	Ambient temperature
Ammonia mass - resultant [kg]	17,889
Physical state	50% liquid
Emission source height [m]	0; 1.15

186

Accepted Article

187 The simulation parameters (Table 2) were selected to indicate different weather conditions in  
 188 order to indicate the differences in emission and the displacement of the plume which  
 189 correspond to summer conditions (30 °C) and winter conditions (-20 °C). Also, the height of  
 190 the emission source influences changes in the emission, therefore three parameters were  
 191 selected from the ground up to 50% of the tank or pipeline height.

192

193 Table 2. Variable parameters used for the simulation for both objects.

Scenario No.	Wind speed and direction [m/s]	The height of emission source [m]	Ambient temperature [°C]	Relative humidity [%]	Atmospheric stability class*
1	1	0	30	50	B
2	1	1.15	30	50	B
3	8	0	30	50	D
4	8	1.15	30	50	D
5	25	0	30	50	D
6	25	1.15	30	50	D
7	1	0	-20	5	B
8	1	1.15	-20	5	B
9	8	0	-20	5	D
10	8	1.15	-20	5	D
11	25	0	-20	5	D
12	25	1.15	-20	5	D

194 \*B: Moderately unstable conditions; D: Neutral conditions

195

196 Wind speed and direction, from 1 to 25 m/s, were selected to present changes and dynamics of  
 197 the spread of pollutants in extreme conditions. In the case of drones up to MTOM (Maximum  
 198 Take-off Mass) of approx. 25 kg, a speed of 25 m/s will be too high, however, for heavier  
 199 structures (above MTOM 25 kg), intended for specialized tasks (including measurements), the  
 200 recommended maximum speed will be adequate.

201 Exposition Guideline Level for ammonia were presented in the table 3. AEGL is calculated for  
 202 five relatively short periods of exposure (10 and 30 min and 1, 4, and 8 h) (Table 3), while  
 203 AEGL "levels" depend on the severity of toxic effects caused by exposure, with level 1 being  
 204 the lowest and level 3 being the most severe (EPA, 2023).

205

206 Table 3. Exposition Guideline Level for ammonia (National Research Council, 2010).

Exposition Level	Unit	Time				
		10 [min]	30 [min]	60 [min]	4 [hr]	8 [hr]
AEGL 1	[ppm]	30	30	30	30	30
AEGL 2	[ppm]	220	220	160	110	110
AEGL 3	[ppm]	2,700	1,600	1,100	550	390

207

208 *2.3. UAV characteristics*

209 There are several types of UAVs used to perform various types of missions and collect data  
 210 using sensors: rotocopters (e.g. multirotors, helicopters), fixed-wing (e.g. aeroplanes), hybrids  
 211 (e.g. VTOL – Vertical Take Off and Landing), aerostates (e.g. balloons), flapping-wing. Each  
 212 of these have advantages and disadvantages verified and widely described in the literature  
 213 (Lambey and Prasad 2021; Gupta et al., 2013; Mustapić et al., 2021). Among these  
 214 constructions, in the authors' opinion, rotocopters should be assigned to the greatest suitability  
 215 for remote measurements of air quality and pollutants. Their greatest advantage is the possibility  
 216 of hovering over the point, which increases the accuracy of measurements, as well as the  
 217 possibility of vertical take-off and landing without the need to provide a runway.

218 It is worth to mention, that use of a UAV equipped with an appropriate RGB (Red Green Blue),  
 219 night vision or thermal camera allows monitoring or recording images, recognizing large areas  
 220 (land or sea), locating suspicious people, vehicles, damaged objects without the need to send a  
 221 patrol there (Bein et al., 2015). Additional support systems such as remote object detection and  
 222 automatic alerting or sending notifications directly to ground patrols support the operational  
 223 work of border guards and increase the efficiency of operations (Greenblatt et al., 2008). To  
 224 describe this concept, the authors decided to use the hexacopter Yuneec Typhoon H520 drone  
 225 equipped with an RGB camera and air pollution analyser ATMON FL. The rationale for this  
 226 choice is that type of UAV is used in scientific research projects for the needs of the Polish  
 227 Border Guard, which has a built-in camera and selected sensors (Table 4). Air pollution analyser  
 228 is cost-effective and easy to deploy.

229

230

231

232

233

234 Table 4. Characteristics of UAS and characteristics of the analyser used during the research.

Parameters	Characteristic
Yuneec Typhoon H520, RGB camera and ground control station	
Weight (with battery and rgb camera)	2 kg
Dimensions	520 x 455 x 295 mm
Flight time	28 minutes
Maximum horizontal velocity	72 km/h
Remote control	ST16S
Maximum flying altitude	500 m
Transmission distance range	1.6 km
RGB camera	E90
Camera resolution	20 megapixel
View field	DFOV 91
Remote control/ground control station	ST16S with 7" HD Touch LCD
Application to planning mission	DataPilot™ Mission Control Software System
Air pollution analyser ATMON FL	
Weight (with battery and RGB camera)	300 g
Dimensions	Ø of enclosure max 125 mm OVERALL DEVICE HEIGHT max 115 mm
Flight time	20 minutes
Transmission distance range	1.6 km
Application to present measurement	ATMON FL GRUND UNIT
Gas/pollution module	NH <sub>3</sub> /ATM-FL-NH3
Reaction time	< 30 s
Accuracy	1 ppm
Measurement range	0-100 ppm
Resolution of measurement	0,01 ppm

235

236 The drone is one of the elements of the tool in question, the aim of which is to optimize actions  
 237 in the event of a failure. Therefore, the parameters characterizing the drone must be adapted to  
 238 other elements, including the parameters of the virtual environment (see chapter 2.4.). The  
 239 ATMON FL used is an independent mobile system for measuring gas and dust air pollutants in  
 240 forced mode. It is intended to be carried by unmanned aerial vehicles (UAV – Drones),  
 241 dedicated to installation on a drone. Detection time of the sensors used to measure ammonia,  
 242 which is integrated with the drone, is < 30 s (Table 4).

243

244

245 2.4. *Virtual environment*

246 In order to better visualise the measurement data and improve making the right decisions (e.g.  
247 relating to evacuation), it will be useful to take advantage of virtual reality technology –  
248 especially in the aspect of the UAV control interface (Kamińska et al., 2019). The implemented  
249 project aims to develop and produce a prototype of an unmanned aircraft control system using  
250 the pilot's eyesight. The developed system offers such functionalities as:

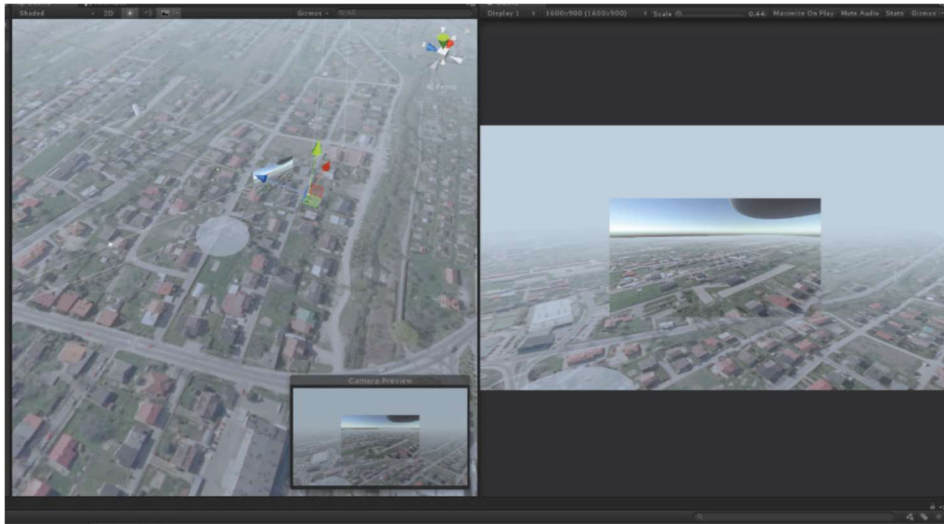
- 251 • taking control of the autonomous UAV flight using goggles as well as controllers,
- 252 • ensuring the issuing of commands and control to the UAV and the camera,
- 253 • the working length of the device is not shorter than the UAV.

254 The prototype of these system consists following elements:

- 255 • multicopter Yuneec H520 with E90 camera,
- 256 • ground control station ST16,
- 257 • Pico Neo2 Eye VR goggles with built-in eye tracking,
- 258 • controllers,
- 259 • notebook.

260 The system requires two remote controls. One operates the Ground Control Station and the  
261 other controls the UAV with the help of goggles and controllers. The pilot in the goggles can  
262 see the view from the drone's camera and the map with the UAV location. The pilot can use his  
263 eyesight to give commands: moving the camera, fly to a set point, stop an ongoing mission,  
264 return to an interrupted mission, change the speed and altitude of the drone. Due to the fact that  
265 the project concerns the sphere of security and defence and was made for the needs of the Border  
266 Guard, some information, including the appearance of the interface, cannot be made public.  
267 What is more, these system may also use virtual reality to display additional information in the  
268 goggles, for example a map of the operational area, what is shown in Fig. 2.

269



270

271 Figure 2. Screen from the prototype of the camera control system (Argasiński et al., 2019;  
 272 Feltynowski 2019).

273

274 Taking into account the calculations and simulations presented in the previous chapter, it should  
 275 be stated that it would be fully justified and advisable to overlay the simulation results on the  
 276 terrain map (for instance on 3D terrain map) seen by the operator.

277

### 278 3. Results

#### 279 3.1. Results of simulation

280 The Figures 3-15 present the simulation results for different parameters (wind speed, the height  
 281 of emission source, ambient temperature, relative humidity) for two objects, i.e., the tank (a)  
 282 and direct source (b).

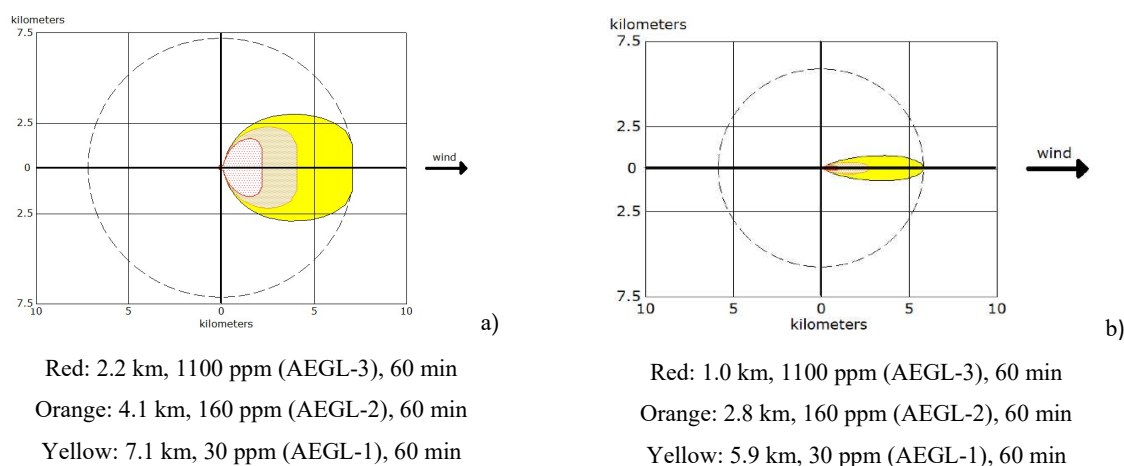


Figure 3. Simulation results – scenario 1 for the parameters: wind speed: 1 m/s, the height of emission source 0 m, ambient temperature 30 °C, relative humidity 50 %, atmospheric stability class B.

283

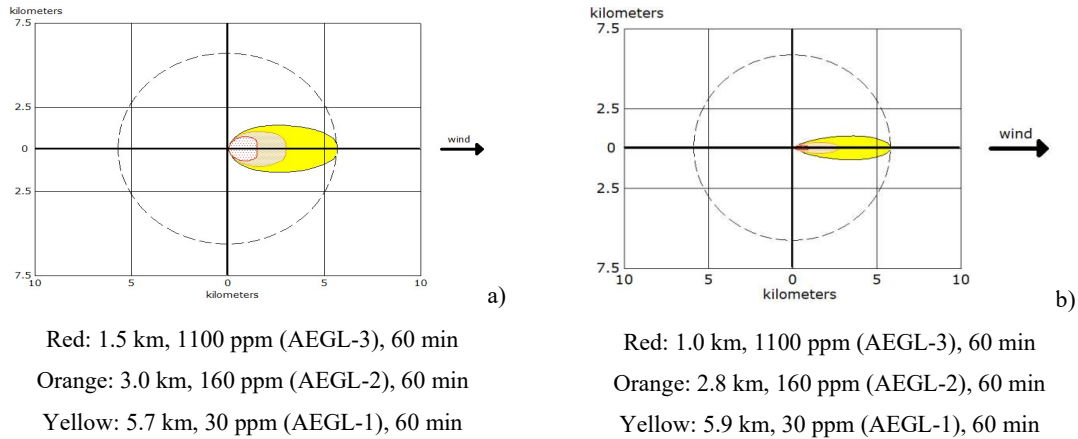


Figure 4. Simulation results – scenario 2 for the parameters: wind speed: 1 m/s, the height of emission source 1.15 m, ambient temperature 30 °C, relative humidity 50 %, atmospheric stability class B.

284

285

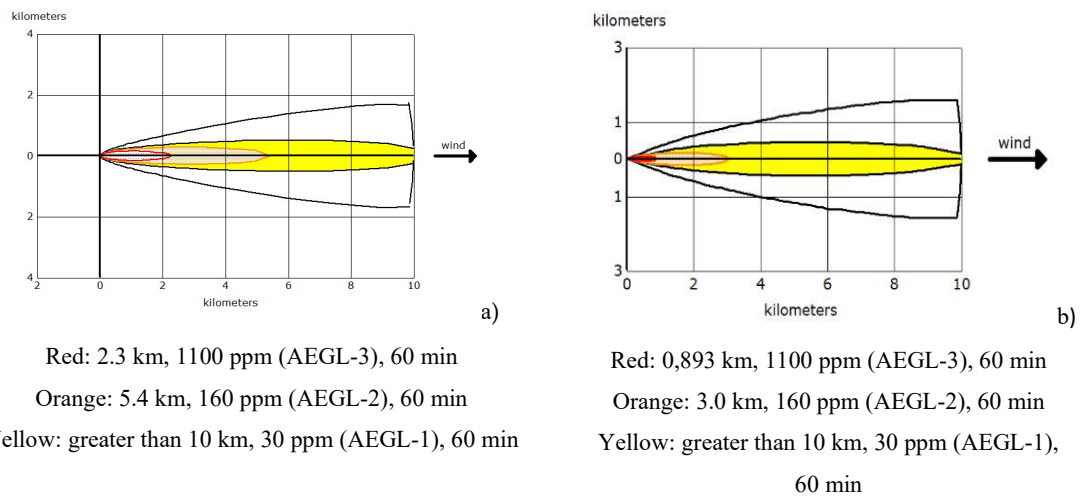
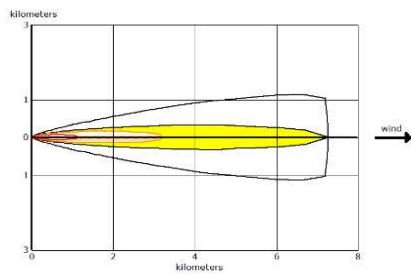


Figure 5. Simulation results – scenario 3 for the parameters: wind speed: 8 m/s, the height of emission source 0 m, ambient temperature 30 °C, relative humidity 50 %, atmospheric stability class D.

286

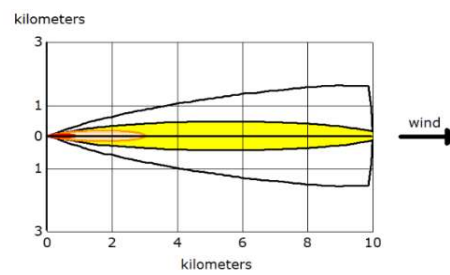
287

288



a)

Red: 1.1 km, 1100 ppm (AEGL-3), 60 min  
 Orange: 3.2 km, 160 ppm (AEGL-2), 60 min  
 Yellow: 7.3 km, 30 ppm (AEGL-1), 60 min



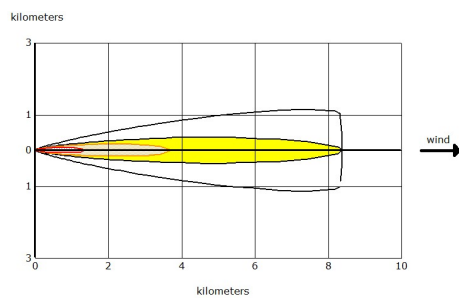
b)

Red: 0,892 km, 1100 ppm (AEGL-3), 60 min  
 Orange: 3.0 km, 160 ppm (AEGL-2), 60 min  
 Yellow: greater than 10 km, 30 ppm (AEGL-1), 60 min

Figure 6. Simulation results – scenario 4 for the parameters: wind speed: 8 m/s, the height of emission source 1,15 m, ambient temperature 30 °C, relative humidity 50 %, atmospheric stability class D.

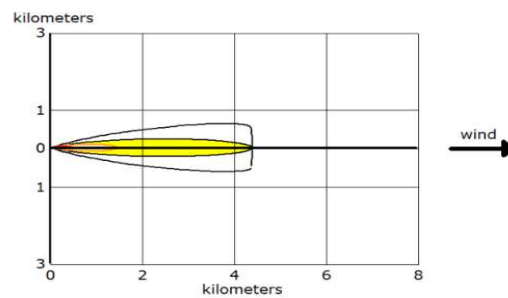
289

290



a)

Red: 1.4 km, 1100 ppm (AEGL-3), 60 min  
 Orange: 3.7 km, 160 ppm (AEGL-2), 60 min  
 Yellow: 8.4 km, 30 ppm (AEGL-1), 60 min



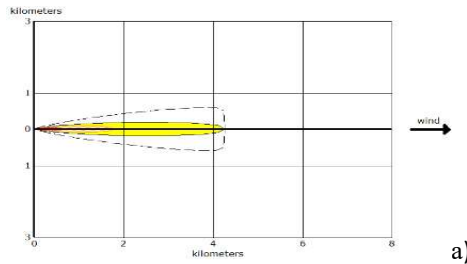
b)

Red: 0,461 km, 1100 ppm (AEGL-3), 60 min  
 Orange: 1.4 km, 160 ppm (AEGL-2), 60 min  
 Yellow: 4.4 km, 30 ppm (AEGL-1), 60 min

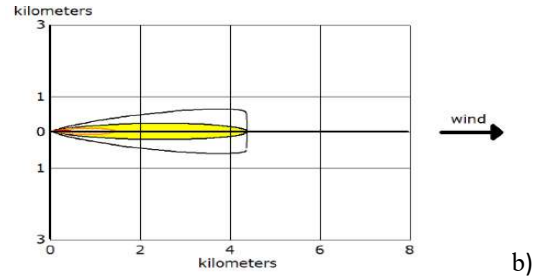
Figure 7. Simulation results – scenario 5 for the parameters: wind speed: 25 m/s, the height of emission source 0 m, ambient temperature 30 °C, relative humidity 50 %, atmospheric stability class D.

291

292



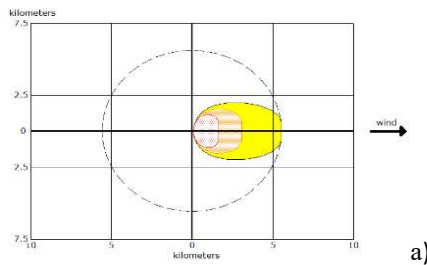
Red: 0,639 km, 1100 ppm (AEGL-3), 60 min  
 Orange: 1.8 km, 160 ppm (AEGL-2), 60 min  
 Yellow: 4.3 km, 30 ppm (AEGL-1), 60 min



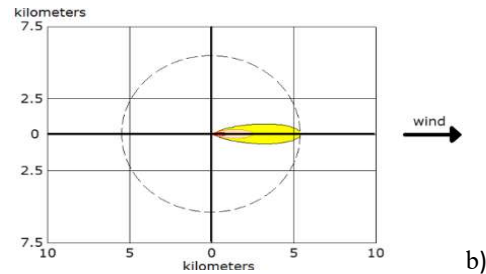
Red: 0,460 km, 1100 ppm (AEGL-3), 60 min  
 Orange: 1.4 km, 160 ppm (AEGL-2), 60 min  
 Yellow: 4.4 km, 30 ppm (AEGL-1), 60 min

Figure 8. Simulation results – scenario 6 for the parameters: wind speed: 25 m/s, the height of emission source 1.15 m, ambient temperature 30 °C, relative humidity 50 %, atmospheric stability class D.

293



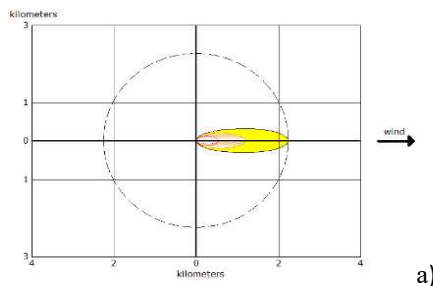
Red: 1.6 km, 1100 ppm (AEGL-3), 60 min  
 Orange: 3.1 km, 160 ppm (AEGL-2), 60 min  
 Yellow: 5.6 km, 30 ppm (AEGL-1), 60 min



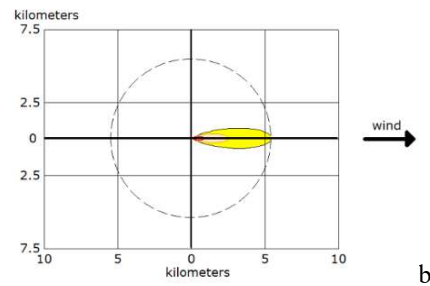
Red: 0,934 km, 1100 ppm (AEGL-3), 60 min  
 Orange: 2.5 km, 160 ppm (AEGL-2), 60 min  
 Yellow: 5.5 km, 30 ppm (AEGL-1), 60 min

Figure 9. Simulation results – scenario 7 for the parameters: wind speed: 1 m/s, the height of emission source 0 m, ambient temperature -20 °C, relative humidity 5 %, atmospheric stability class B.

294



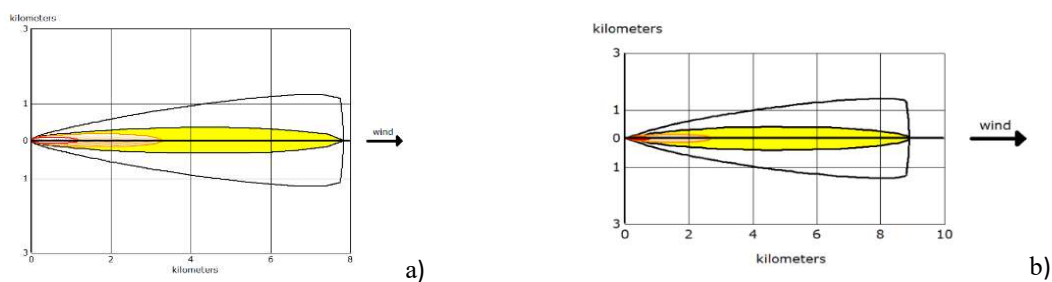
Red: 0,539 km, 1100 ppm (AEGL-3), 60 min  
 Orange: 1.2 km, 160 ppm (AEGL-2), 60 min  
 Yellow: 2.3 km, 30 ppm (AEGL-1), 60 min



Red: 0,934 km, 1100 ppm (AEGL-3), 60 min  
 Orange: 2.5 km, 160 ppm (AEGL-2), 60 min  
 Yellow: 5.5 km, 30 ppm (AEGL-1), 60 min

Figure 10. Simulation results – scenario 8 for the parameters: wind speed: 1 m/s, the height of emission source 1,15 m, ambient temperature -20 °C, relative humidity 5 %, atmospheric stability class B.

295



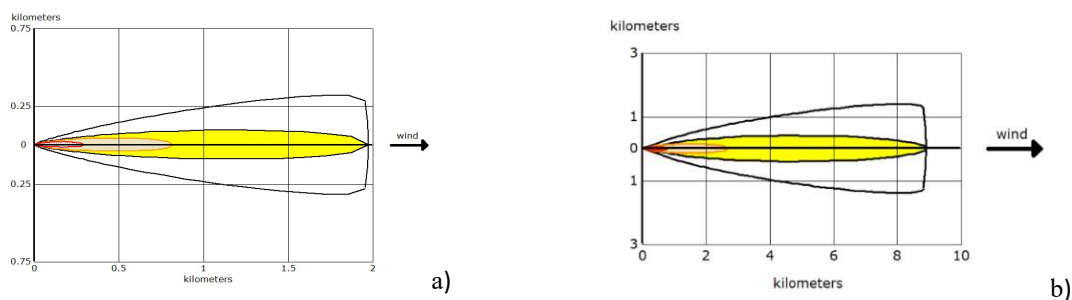
Red: 1.2 km, 1100 ppm (AEGL-3), 60 min  
 Orange: 3.3 km, 160 ppm (AEGL-2), 60 min  
 Yellow: 7.8 km, 30 ppm (AEGL-1), 60 min

Red: 0,802 km, 1100 ppm (AEGL-3), 60 min  
 Orange: 2.7 km, 160 ppm (AEGL-2), 60 min  
 Yellow: 8.9 km, 30 ppm (AEGL-1), 60 min

Figure 11. Simulation results – scenario 9 for the parameters: wind speed: 8 m/s, the height of emission source 0 m, ambient temperature -20 °C, relative humidity 5 %, atmospheric stability class D.

296

297



Red: 0,295 km, 1100 ppm (AEGL-3), 60 min  
 Orange: 0,819 km, 160 ppm (AEGL-2), 60 min  
 Yellow: 2.0 km, 30 ppm (AEGL-1), 60 min

Red: 0,802 km, 1100 ppm (AEGL-3), 60 min  
 Orange: 2.7 km, 160 ppm (AEGL-2), 60 min  
 Yellow: 8.9 km, 30 ppm (AEGL-1), 60 min

Figure 12. Simulation results – scenario 10 for the parameters: wind speed: 8 m/s, the height of emission source 1,15 m, ambient temperature -20 °C, relative humidity 5 %, atmospheric stability class D.

298

299

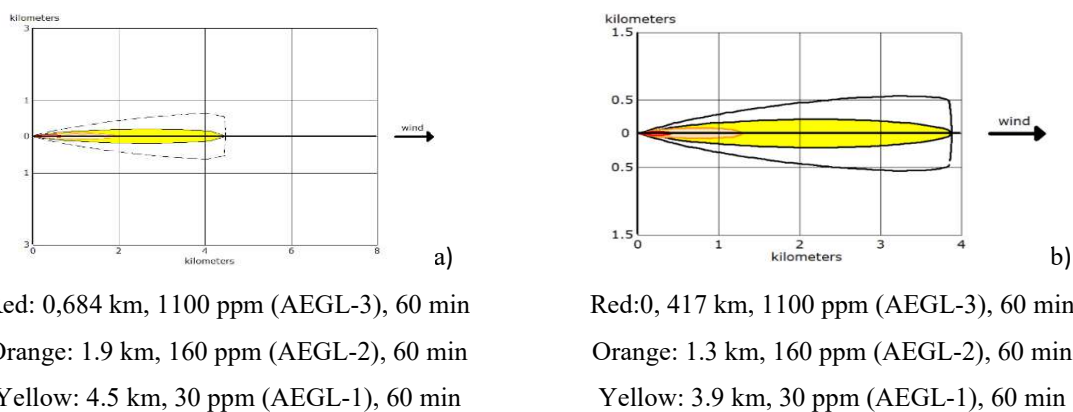


Figure 13. Simulation results – scenario 11 for the parameters: wind speed: 25 m/s, the height of emission source 0 m, ambient temperature -20 °C, relative humidity 5 %, atmospheric stability class D.

300

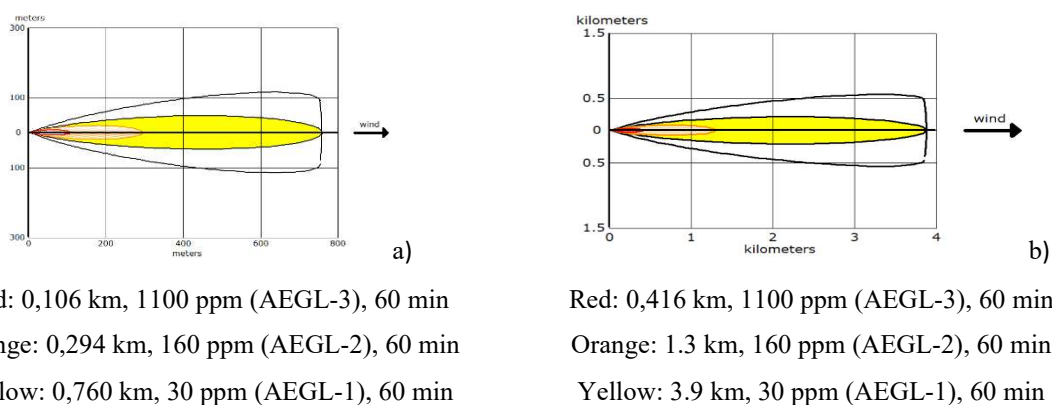


Figure 14. Simulation results – scenario 12 for the parameters: wind speed: 25 m/s, the height of emission source 1,15 m, ambient temperature -20 °C, relative humidity 5 %, atmospheric stability class D.

## 301 4. Discussion

### 302 4.1. ALOHA simulation

303 The ALOHA program allowed for the analysis of the migration trajectory of the toxic gas  
 304 ammonia for two selected cases, including emissions from a tank of given dimensions (diameter  
 305 2.3 m, length 13.4 m, capacity 55,674 dm<sup>3</sup>) filled with 50% NH<sub>3</sub>. The simulation of emissions  
 306 from a tank that has become unsealed, e.g., during transport, takes into account the height of  
 307 the emission source, the rate of ammonia release and changes in the gas content in the tank, and  
 308 the range of impact. The simulations included 12 different scenarios in which the variable  
 309 parameters were: wind speed, emission source height, ambient temperature, relative humidity  
 310 and the atmosphere stability class (Table 2). In the case of temperature, the analysis covered  
 311 two extreme cases, i.e., summertime with a temperature of 30°C and winter time with a

312 temperature of  $-20^{\circ}\text{C}$ . It should be added, that the choice of temperature is important not only  
313 for the simulation process, but also for the selection of sensors used for the analysis. The sensors  
314 used to analyse ammonia concentration must operate in a given temperature range. It is  
315 important that measurement accuracy is maintained, acceptable to the operator. Appropriate  
316 sensor response time and sending information about the analyte concentration are also  
317 necessary. The analyser selected by the authors had a time of less than 30 s which allowed  
318 obtaining information in real time.

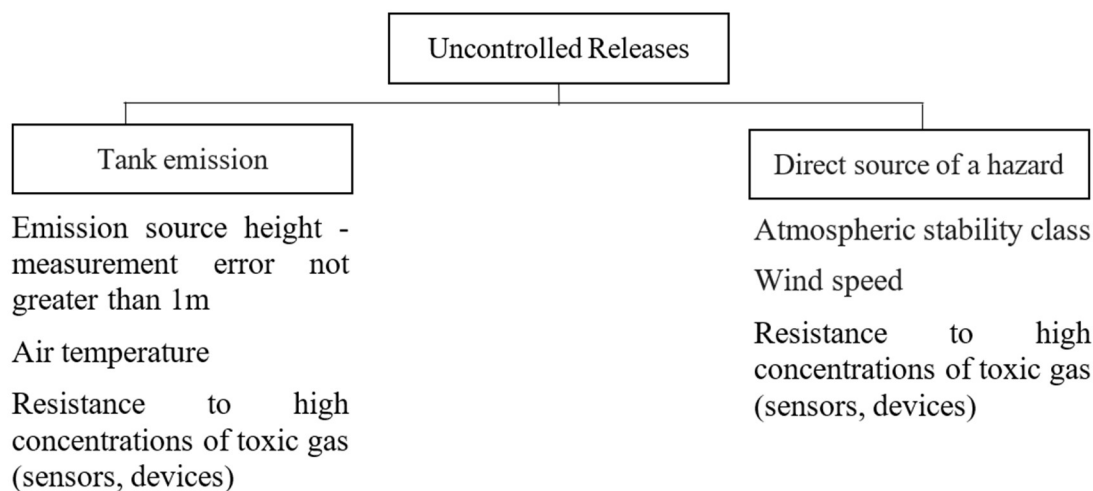
319 Ammonia is stored in a liquid state under pressure. Any time the ammonia container is opened,  
320 it may leak. The performed calculations allowed to determine the extent of the toxic cloud with  
321 a concentration above the threshold value and the direction of its movement (Fig. 3-14). Based  
322 on the data entered into the program and the adopted assumptions (Tables 1 and 2), the analysis  
323 of the effects resulting from the release of  $\text{NH}_3$  into the environment was performed. In the first  
324 scenario (Fig. 3), the highest concentration of 1100 ppm and corresponding to AEGL-3 is be  
325 within 2 km from the source, the lower than 160 ppm (AEGL-2) at 3.7 km and the lowest  
326 concentration equal to 30 ppm (AEGL-1) at a distance of 6.5 km. The distribution of pollutants  
327 was obtained for a summer day characterised by relative humidity at the level of 50 %, wind  
328 speed of 1 [m/s], atmosphere stability class B and emission at the height of 0 [m] (Fig. 3). In  
329 the case of a winter day with a temperature of  $-20^{\circ}\text{C}$  (Fig. 9), the scope of the cloud's influence  
330 is smaller and amounts to 1.6, 3.1 and 5.6 km, respectively. People in the AEGL-1 zone (Fig.  
331 1; Table 3) are exposed to ammonia concentrations above which predictably general population  
332 may experience discomfort, irritation or some asymptomatic contamination effects. All of these  
333 effects are transient and reversible, but for those with weaker condition can lead to serious  
334 consequences. In the AEGL-2 zone, which is characterized by an  $\text{NH}_3$  concentration above  
335 which the general population may not only experience irreversible or severe long-term adverse  
336 health effects, but also the ability to evacuate by itself may be deteriorated. The presence of  
337 people in the AEGL-3 zone may pose an immediate threat to life or death. It should be noted  
338 that the individual sensitivity of people and the value of the standard adopted in the European  
339 Union, the TLV (threshold limit value) value of ammonia, as a weighted average value for an  
340 8-hour working day, was set at 19.74 ppm ( $14 \text{ mg/m}^3$ ), and the TLV-STEL (threshold limit  
341 value - short term exposure limit) value at the level of 39.48 ppm ( $28 \text{ mg/m}^3$ ) (Neghab et al.,  
342 2018). The maximum dose to which each person within 100 m of the place where  $\text{NH}_3$  is  
343 released from the tank during the first hour is exposed is 10 kg/min at  $30^{\circ}\text{C}$  and 3 kg/min at -  
344  $20^{\circ}\text{C}$  (Fig. 3, Fig. 9).

345 Selecting the Source Strength option in the ALOHA program gives the possibility to present  
346 the amount of a chemical substance that is released from the tank as a function of time, i.e., the  
347 determination of the "source's firepower". Information in this regard is important for people  
348 staying at the place of the leak. The obtained results allowed to determine the accuracy with  
349 which it is necessary to transmit information from the drone to the centre in order to verify  
350 changes in the pollution stream due to e.g. changes in wind speed. In the case of the simulation  
351 for the same temperature (i.e. 30 °C, Fig 3-8, or -20 °C, Fig. 9-14), it was shown that the  
352 accuracy of the measurement of the height of the emission point of the substance cannot be less  
353 than 1 m. Lack of accuracy in this range significantly affects the assessment of both the  
354 ammonia release rate and the size of the streak. If the emission occurs at a height of 1.15 m,  
355 the impact range is smaller, while the change in wind speed is not that significant. The use of  
356 a drone allows for direct verification of data in real time. Information about the analysed  
357 parameters is transferred from the drone to the management point on an ongoing basis (the  
358 response time of the analyser is less than 30 s), which allows updating the simulation of the  
359 spread of pollution and taking action in the area which becomes contaminated. The use of a  
360 monocular (Fig. 2, Fig. 19) allows to control the drone while ensuring the safety of the drone  
361 operator. Comparing the obtained simulation results for the emission situation from the 0 m  
362 point and for the 1.15 m point (Fig. 3-14), it can be noticed that the wind speed and the stability  
363 of the atmosphere are of great importance in the event of a crisis situation such as unsealing of  
364 the tanker during transport. It requires appropriate and quick action of the services.

365 With regard to emissions from a fixed point (e.g. from the pipeline), the results obtained indicate  
366 a significant influence of parameters such as wind speed and temperature on air pollution, as  
367 well as the amount of pollutants emitted, humidity and the atmosphere stability class. Comparing  
368 the results obtained for the same atmospheric conditions, but with a different heights of the  
369 emission point, it can be seen that the emission source height is not as critical parameter as in  
370 the case of emissions from the tank. The change of height under the same weather conditions  
371 gives the same range of impact of ammonia. This is a consequence of the assumptions and  
372 processes included in the ALOHA. It should also be noted that the form in which ammonia will  
373 be transported through a pipeline or in a tank also determines the processes it will undergo  
374 immediately after release.

375 Analysing the influence of temperature on the spread of the ammonia cloud, it can be noticed  
376 that the temperature also does not play a significant role in the analysis. Both at 30 °C and -20  
377 °C, comparable results of the spread of the released pollutant were obtained. It should be noted,  
378 however, that in the case of the scenarios analysed for the winter period, it was noted that the

379 impact range is slightly smaller than for the summer period. This is, of course, related to the  
 380 reflection of the spread of gases depending on temperature and humidity.  
 381 The analysis of the results obtained shows that, depending on the type of failure, it is necessary  
 382 to take into account the appropriate variables that affect the accuracy and safety of firefighters  
 383 and other participants in the action (Fig. 15).



384

385 Figure 15. Selection of parameters depending on the type of event.

386

387 The results obtained correlate well with the literature data showing that the models developed  
 388 as a result of simulations in the ALOHA environment are a very good support for the process  
 389 of managing the risk of high hazards related to the release of dangerous gases into the  
 390 atmosphere. They facilitate the selection of the optimal solution for a given event (Jones et al.,  
 391 2013). For example, a simulation of the release of chlorine, epichlorohydrin and phosgene from  
 392 storage tanks located at three factories in a chemical complex in central Taiwan was performed  
 393 to obtain the results necessary to develop the scenarios according to the emergency response  
 394 planning guidelines (ERPG) and their corresponding values directly dangerous to life or health  
 395 (IDLH – dangerous to life or health) (Tseng et al., 2012). The simulations took into account the  
 396 wind speed, the level of atmospheric stability and the total release time. The simulation results  
 397 were used as a basis for gas leak analysis and risk assessment.

398 The use of the ALOHA environment was also used to simulate failures in order to prepare crisis  
 399 management scenarios. For example, Orozco et al. (2019) obtained a model of the quantitative  
 400 impact on humans and the environment in the event of ammonia release from tanks in the  
 401 Matanzas industrial area, Cuba (Orozco et al., 2019). Thanks to the use of ALOHA software,  
 402 various scenarios were obtained: "Toxic vapor cloud", "Flammable area" and "Vapour cloud  
 403 explosion", and the number of victims was determined in the event of each scenario occurring.

404 Also Nandu and Soman (2018) performed a hypothetical release of liquid ammonia from a  
405 chemical plant warehouse based on CFD (Computational Fluid Dynamics) analysis, and the  
406 dispersion of ammonia vapor in the atmosphere using ALOHA (Nandu and Soman., 2018). The  
407 results obtained by James (2015) indicate that as the wind speed increases, the danger zone  
408 decreases, because as the wind speed decreases, the period of formation of vapor clouds  
409 lengthens and the density of ammonia vapours in the atmosphere increases. The maximum risk  
410 zone calculated as a result of the simulation was obtained for a wind speed of 4 m/s. Ammonia  
411 concentrations were higher than its MRL of 25 ppm for distances of up to 5 km at a wind speed  
412 of 4 m/s. One of the main hazards in petrochemical plants is ammonia leakage. Based on the  
413 results of the HAZOP (hazard and operability) study, ammonia emissions were modelled at the  
414 petrochemical plant in Asaluyeh (Iran) (Abbaslou and Karimi, 2019). The three most likely  
415 accident scenarios were selected, including a toxic vapor cloud, a jet fire and a boiling liquid  
416 vapor expanding explosion (BLEVE). Then, scenario modelling was performed using the  
417 ALOHA environment. The toxic vapor cloud scenario assumes the release of 81,316 kg of  
418 ammonia. The concentration of toxic ammonia fumes exceeded 1,100 ppm at a distance of 1  
419 km, causing death within 60 seconds. Overpressure never exceeds 3.5 psi; so it shall not cause  
420 serious injuries or damage to buildings. In the third scenario, BLEVE's thermal radiation  
421 exceeds  $10 \text{ kW/m}^2$  at an altitude of 376 m and can cause death within 60 seconds (Abbaslou  
422 and Karimi, 2019).

423 In the case of the ammonia release analysis presented in the article, conducting a simulation in  
424 the initial phase of the threat using the ALOHA model would not only be useful for the rescue  
425 commander, but also beneficial for the residents of the affected areas by letting them know  
426 about necessary precautions to ensure the safety of their lives and property.

427 The use of the ALOHA model, as indicated by the results of the authors and other researchers,  
428 is a good and simple tool that allows for proper management in case of contamination threat. It  
429 can, therefore, be used as a support tool in activities aimed at protecting human health and  
430 environmental protection against hazardous gases, such as ammonia. However, it should be  
431 noted that each case must be considered individually, e.g., due to different atmospheric  
432 conditions analysed or the characteristics of the container from which the release takes place.

433

#### 434 *4.2. The use of drones and virtual reality*

435 Comparing the obtained results for both systems, it should be stated that in the event of an  
436 accident, such as emission of the harmful substance from the tank during transport (e.g.  
437 ammonia) each one element included in the ALOHA program is important and determines the

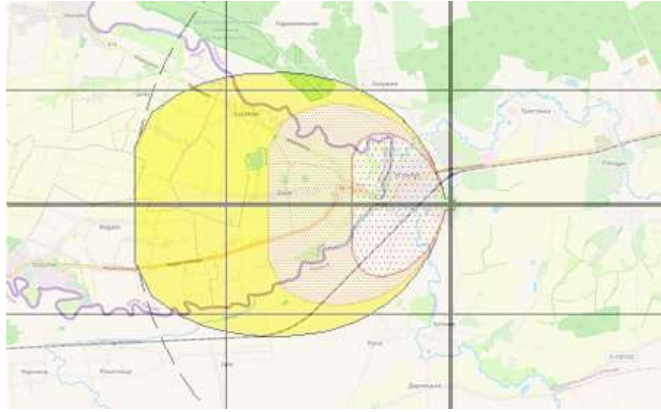
438 formation of a cloud. Taking into account the fact that in such situations it is very often  
439 impossible to directly analyse the release rate, the temporary change in the concentration of  
440 ammonia in the air and its spread in the environment, the use of simulation methods in  
441 combination with drones is an indispensable tool for quicker threat assessment. Using the  
442 simulation results, with the assumed parameters of the atmosphere and the emission source, we  
443 obtain information about the possible path of pollution migration. The person managing the  
444 rescue operation, in the situation of gas release, through drones has the ability to track the streak  
445 and make appropriate changes to the program in order to obtain the cloud that best corresponds  
446 to the real changes taking place in the environment. It is very important that the tool is easy to  
447 apply and interpret, without high hardware requirements, and can be used in the field. The  
448 ALOHA program belongs to this type of program. The data obtained from the simulation allows  
449 then the UAV to be sent for verification and ongoing monitoring of the moving plume in the  
450 air. The drone, thanks to the installed appropriate sensors (Rabajczyk et al., 2020), enables the  
451 qualitative and quantitative measurement of selected air pollution.

452 In order to properly implement actions in the situation of failure and release of hazardous gas,  
453 it was assumed to use an unmanned aerial vehicle (with an appropriate measuring system) in  
454 accordance with the following concept:

- 455 1) fly over the cloud of substances,
- 456 2) make the quantitative-quality measurement of pollution from the cloud of gas,
- 457 3) locate a place of the (unsealing, gaps, holes), assess its size,
- 458 4) send data from the measurement and size of the leak to the simulation,
- 459 5) make a simulation based on the data provided by the drone.

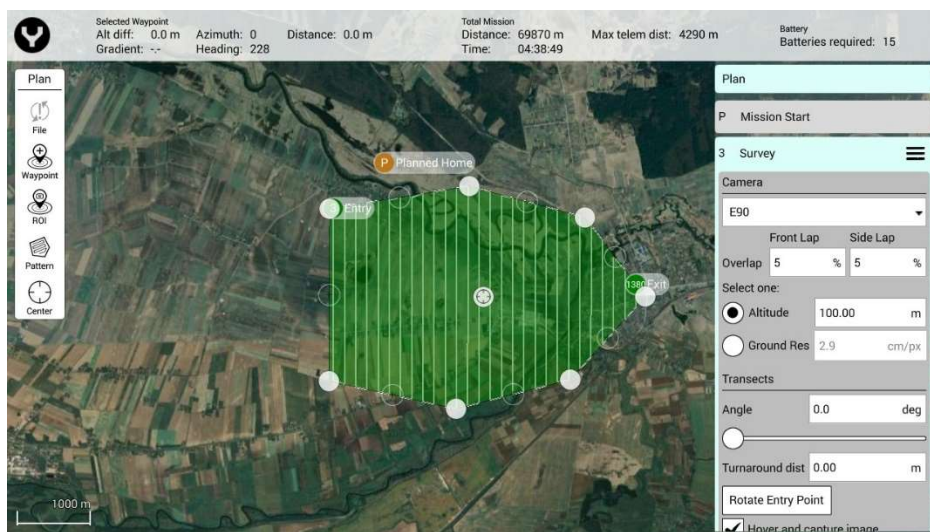
460 In order to illustrate the advantages of simulation, scenarios no 1. was selected for the analysis  
461 of tank failure cases. Next, a compilation of the simulation results from ALOHA on a map of  
462 sparsely populated area was made (Fig. 16).

463



464  
 465 Figure 16. Compilation of results of simulation scenario no 1. and map of sparsely populated  
 466 area (correct scale or proportions are maintained).

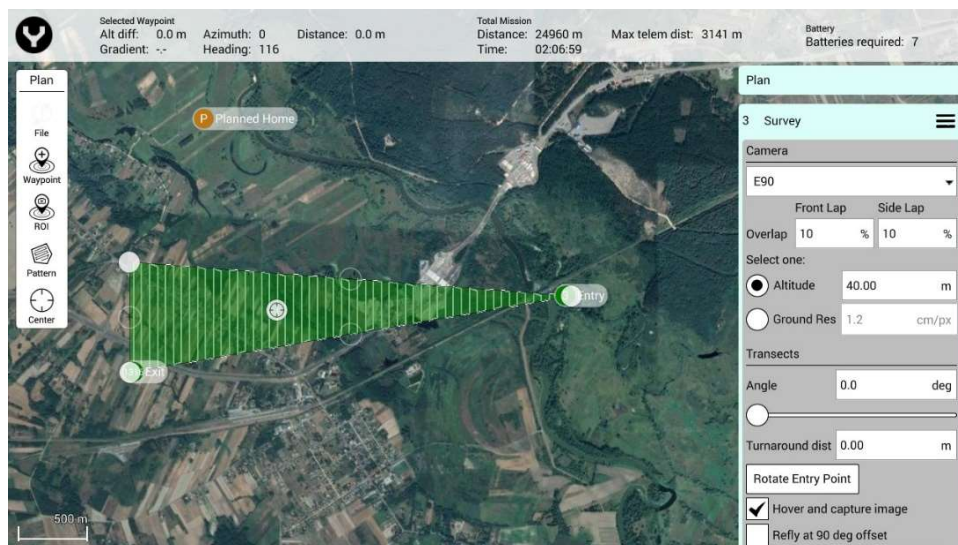
467  
 468 As shown in the figure above, the authors have obtained a picture of a specific areas exposed  
 469 to the result of leaks. Thus, it is now possible to plan the optimal route for the UAV, coverage  
 470 path. Knowing the size and shape of area affected by leakage, it will also be possible to calculate  
 471 how many batteries in UAV will be needed to complete the entire mission, and how long it  
 472 takes. The limitation of performed simulations is that they do not include the estimated height  
 473 of the leakages. Thus, the pilot has to decide from what height a measurement should be started.  
 474 As mentioned, a simulation of a specific areas exposed to the result of a leak was obtained. It  
 475 allows to arrange the appropriate shape of the flight route and plan the mission. Below figure  
 476 (Fig. 17) presents proposed flight path for simulation scenario no 1. The flight altitude was  
 477 assumed to be 100 m. The planned mission shows that total time of mission is 4 hours and 38  
 478 minutes. What is more, to complete the flight up to 15 batteries are required.



479  
 480 Figure 17. Proposed flight path for simulation scenario no 1. Source: DataPilot™ Mission  
 481 Control Software System

Accepted Article

482 Next figure (Fig. 18) presents proposed flight path for simulation scenario no 12. The flight  
483 altitude was assumed to be 40 m, because the height of buildings is lower than in scenario no.1.  
484 The planned mission shows that total time of mission is 2 hours and 06 minutes. What is more,  
485 to complete the flight up to 7 batteries are required.



486  
487 Figure 18. Proposed flight path for simulation scenario no 12. Source: DataPilot™ Mission  
488 Control Software System

489  
490 The above simulations give grounds for the statement that total time of mission is relatively  
491 long. It seems that such long-term measurement is not conducive to quick response and  
492 planning of rescue and crisis management actions. Thus, it is recommended to establish shorter  
493 path, to divide the area into smaller sectors and use several independent drones controlled by  
494 pilots at the same time. However, due to the analyser ATMON FL, the use of a drone swarm is  
495 preferred.

496 Should be noted that in this simulation, atmospheric conditions were not taken into account,  
497 because DataPilot™ Mission Control Software System does not have such features and does  
498 not take into account, e.g., the wind speed, humidity, air temperature when calculating the  
499 required batteries. Moreover, the maximum distance for telemetry exceeds the range of the  
500 ground control station ST16S as well as air pollution analyser ATMON FL, so the pilot should  
501 have to follow the UAV in order to maintain connection and not to lose radio link.

502 Simulation results obtained from the ALOHA program also indicate that it is important for the  
503 operator's safety to select the analyzer appropriately to the prevailing weather conditions. If the  
504 range is too small, the operator may be exposed to contamination.

505 The system has been thoroughly tested to adapt its functionalities and capabilities to the needs  
506 and requirements of users (firefighters, border guards, rescue services). The prototype of such

507 a system was tested by the project team from July till August 2021. Tests of the system are  
508 shown in Fig. 19.

509



510 a) b)  
511 Figure 19. Photos from tests (Authors: Zawistowski, Kęty, 2021 (a); Florek, Duchnow, 2021  
512 (b)).

513

514 Therefore, combining drone operation with predictions of pollution migration from modelling  
515 showed limitation and challenges using UAV and demonstrated what parameters may be  
516 important for such application (for example: UAV wind resistance, data transmission range,  
517 possibility of using the vehicle with a docking station). The combination of both tools, i.e., a  
518 drone guided by a pilot using his eyes, and the ALOHA program, allows for proper management  
519 of the drone, taking action in the contaminated area, and adapting work in the event of a change  
520 in weather conditions.

521 The pilot should also be aware of the uncertainties resulting from the simulation, as this will  
522 allow him to plan the mission parameters so as to properly scan the area, e.g., knowing the  
523 direction of movement, knows where the UAV should fly and in which area (surface) to check  
524 concentrations at different heights in order to detect contamination. It should be added, that the  
525 uncertainty is related to the accuracy of the input data used for the simulation. The change in  
526 weather conditions determines the accuracy of the simulation. Therefore, the use of a drone and  
527 real-time data verification allows for the reduction of simulation uncertainty and allows  
528 obtaining reliable information necessary for the proper conduct of the action and react to  
529 changes occurring in real time.

530 The development of the concept itself showed that thanks to the performed simulations based  
531 on the assumed parameters (ALOHA), at the stage of planning it was found that technical  
532 (planned route, range of data transmission) and logistical (follow the UAV to not lose radio  
533 link) issues must be solved. The UAV flight route planning should take into account weather  
534 conditions (including wind speed and direction, humidity, air temperature).

535

536 **5. Conclusions**

537 Substances present in the atmosphere have an impact on human health and environmental  
538 safety. At the same time air pollution can spread anywhere and cannot be limited to a selected  
539 area. Especially all kinds of uncontrolled emissions of hazardous gases (such as ammonia) can  
540 create critical situations.

541 Based on the analyses, the authors identified the need for applying virtual reality in combination  
542 with modelling, simulation of impurities migration and the use of UAS in detecting hazardous  
543 gas leaks. It is worth noting that the purpose of application UAS and simulation by ALOHA is  
544 twofold: to create procedures or recommended practices of using drones, as well as, to provide  
545 reliable data for simulation in real-time.

546 Firstly, the use of simulation allows not only a safe (because it is carried out in virtual reality)  
547 testing of scenarios, but also a development of the tactics of using UAS as well as the rules of  
548 observation and measurement. The simulation results may be helpful to determine a number of  
549 drone flight parameters (with sensors attached), which includes but are not limited to:

- 550 - recommended flight altitude depending on the type of released substance,
- 551 - safe distance from the substance cloud,
- 552 - speed at which the drone should move to "keep up" with the cloud.

553 Thus, knowing the distribution of the substance in the cloud and its size, the operator will know  
554 how close he may fly. Moreover, by specifying the distance, the operator will be able to select  
555 a camera to the desired resolution and zoom. In that way, thanks to simulation in a virtual  
556 reality, it is possible to create appropriate procedures, recommended practices, and finally drone  
557 flight rules for the purposes of monitoring the movement of a cloud of a dangerous substance.  
558 Additionally, the possibility of eyes use to drone control allows to ensure the pilot's safety.

559 The presented concept justifies the need to develop comprehensive automated systems that  
560 would allow to simulate the leakage area in 3D and at the same time allow for the determination  
561 of UAV flight routes taking into account the direction and strength of the wind, humidity and  
562 air temperature. This could help to develop a flight path that corresponds as much as possible  
563 to the actual area of the leak and gas movement.

564

565 **Acknowledgements:** This research was co-funded by the National Centre for Research and  
566 Development as part of the project entitled "Controlling an autonomous drone using goggles  
567 (monocular)", no. DOB-BIO9/26/04/2018.

568

569 **Conflicts of Interest:** The authors declare that they have no known competing financial  
570 interests or personal relationships that could have appeared to influence the work reported in  
571 this paper.

572

## 573 **References**

574 Abbaslou H., Karimi A., 2019. Modeling of Ammonia Emission in the Petrochemical Industry.

575 *Jundishapur J Health Sci.*, 11, e94101. <https://doi.org/10.5812/jjhs.94101>

576 Acute Exposure Guideline Levels for Selected Airborne Chemicals: Volume 20. National  
577 Academies of Sciences, Engineering, and Medicine. Washington, DC: The National Academies  
578 Press. 2016. <https://doi.org/10.17226/23634>

579 AIRBEAM - AIRBorne information for Emergency situation Awareness and Monitoring  
580 <https://cordis.europa.eu/project/id/261769> (accessed on 17 February 2022)

581 Al Fayez F., Hammoudeh M., Adebisi B., Abdul Sattar K.N., 2019. Assessing the effectiveness  
582 of flying ad hoc networks for international border surveillance. *International Journal of*  
583 *Distributed Sensor Networks*, 15(7), 1550147719860406, pp. 4.  
584 doi:10.1177/1550147719860406

585 Argasiński, J., Lipp N., Dużmańska-Misiarczyk N., Lesicki Ł., Strojny P., 2019. The use of VR  
586 simulators for training operators and operation of UAV platforms. [in:] Feltynowski M, The  
587 use of unmanned aerial platforms in operations for public safety. CNBOP-PIB, Józefów, pp.  
588 149.

589 Bai Z., Dong Y., Wang Z., Zhu T., 2006. Emission of ammonia from indoor concrete wall and  
590 assessment of human exposure. *Environ. Int.*, 32, 303–311.  
591 <https://doi.org/10.1016/j.envint.2005.06.002>

592 Batstone D.J., Puyol D., Flores-Alsina X., Rodríguez J., 2015. Mathematical modelling of  
593 anaerobic digestion processes: applications and future needs. *Reviews in Environmental Science*  
594 *and Bio/Technology*, 14(4), 595–613. doi:10.1007/s11157-015-9376-4

595 Battye W., Aneja V.P., Roelle P.A., 2003. Evaluation and improvement of ammonia emissions  
596 inventories. *Atmos. Environ.*, 37, 3873–3883. [https://doi.org/10.1016/S1352-2310\(03\)00343-1](https://doi.org/10.1016/S1352-2310(03)00343-1)

597 Bein D., Bein W., Karki A., Madan B.B., 2015. Optimizing Border Patrol Operations Using  
598 Unmanned Aerial Vehicles. *12th International Conference on Information Technology - New*  
599 *Generations*, 13-15.04.2015. Las Vegas, NV, USA., 479-484. doi:10.1109/itng.2015.83

600 Bessagnet B., Menut L., Lapere R., Couvidat F., Jaffrezo J.-L., Mailler S., Favez O., Pennel R.,  
601 Siour G., 2020. High Resolution Chemistry Transport Modeling with the On-Line CHIMERE-  
602 WRF Model over the French Alps-Analysis of a Feedback of Surface Particulate Matter

- 603 Concentrations on Mountain Meteorology. *Atmosphere*, 11(6), 565.  
604 doi:10.3390/atmos11060565
- 605 Bhattacharya R., Kumar G., 2015. Consequence analysis for simulation of hazardous chemicals  
606 release using ALOHA software. *Int J ChemTech Res.*, 8, 2038-2046. Corpus ID: 212489461
- 607 Bittman S., Jones K., Vingarzan R., Hunta D.E., Sheppard S.C., Tait J., So R., Zhao J., 2015.  
608 Weekly agricultural emissions and ambient concentrations of ammonia: Validation of an  
609 emission inventory. *Atmos. Environ.*, 113, 108-117.  
610 <http://dx.doi.org/10.1016/j.atmosenv.2015.04.038>
- 611 Burgués J., Marco S., 2020. Environmental chemical sensing using small drones: A review.  
612 *Science of The Total Environment* 141172. doi:10.1016/j.scitotenv.2020.141172
- 613 CAMELOT - C2 Advanced Multi-domain Environment and Live Observation Technologies  
614 <https://cordis.europa.eu/project/id/740736> (accessed on 17 February 2023)
- 615 COMPASS2020 - Coordination Of Maritime assets for Persistent And Systematic Surveillance  
616 <https://cordis.europa.eu/project/id/833650> (accessed on 17 February 2023)
- 617 EPA, Acute Exposure Guideline Levels for Airborne Chemicals, <https://www.epa.gov/aegl>  
618 (accessed on 17 February 2023)
- 619 Everts S., Davenport M., 2016. Drones detect threats such as chemical weapons, volcanic  
620 eruptions. *Chemical & Engineering News. Environment.*, 94(9), 36-37.  
621 <https://cen.acs.org/articles/94/i9/Drones-detect-threats-chemical-weapons.html> (accessed on  
622 17 February 2023)
- 623 Feltynowski M., 2019. The use of unmanned aerial platforms in operations for public safety.  
624 CNBOP-PIB. ISBN: 978-83-948534-6-4, pp. 24. DOI: 10.17381/2019.1
- 625 Ferlin M., Kurela M., Monge O., Castgnet C., 2019. Smart Operations in ATEX RLV  
626 Environment. *8TH EUROPEAN CONFERENCE FOR AERONAUTICS AND SPACE*  
627 *SCIENCES (EUCASS)*. 1-4 July 2019, Madrid, Spain. 1-13. DOI: 10.13009/EUCASS2019-518
- 628 Fu H., Luo Z., Hu S., 2020. A temporal-spatial analysis and future trends of ammonia emissions  
629 in China. *Sci. Total Environ.*, 731, 138897. <https://doi.org/10.1016/j.scitotenv.2020.138897>
- 630 GAZ SYSTEM. Sustainable Development Report. 2018.  
631 [https://unstats.un.org/sdgs/files/report/2018/thesustainabledevelopmentgoalsreport2018-](https://unstats.un.org/sdgs/files/report/2018/thesustainabledevelopmentgoalsreport2018-en.pdf)  
632 [en.pdf](https://unstats.un.org/sdgs/files/report/2018/thesustainabledevelopmentgoalsreport2018-en.pdf) (accessed on 28 October 2023)
- 633 Giannakis E., Kushta J., Bruggeman A., Lelieveld J., 2019. Costs and benefits of agricultural  
634 ammonia emission abatement options for compliance with European air quality regulations.  
635 *Environ. Sci. Eur.* 31, 93. <https://doi.org/10.1186/s12302-019-0275-0>

- 636 Giompapa S., Farina A., Gini F., Graziano A., di Stefano R., 2007. Computer simulation of an  
637 integrated multi-sensor system for maritime border control. *2007 IEEE Radar Conference*. 17-  
638 20 April 2007, Waltham, Massachusetts. 308-313. doi:10.1109/radar.2007.374233
- 639 Greenblatt A., Panetta K., Agaian S., 2008. Border crossing detection and tracking through  
640 localized image processing. *2008 IEEE Conference on Technologies for Homeland Security*.  
641 12-13 May 2008. Waltham, MA. 333-338. doi:10.1109/ths.2008.4534473
- 642 Gupta S.G., Ghonge M.M., Jawandhiya P.M., 2013. Review of unmanned aircraft system  
643 (UAS). *International journal of advanced research in computer engineering & technology*  
644 (*IJAR CET*), 2(4), 1646-1658.
- 645 Hanna S.R., Briggs G. A., Hosker Jr, R.P., 1982. Handbook on atmospheric diffusion. National  
646 Oceanic and Atmospheric Administration, Oak Ridge, TN (USA). *Atmospheric Turbulence and*  
647 *Diffusion Lab.*, DOE/TIC-11223 ON: DE82002045.
- 648 Hiemstra P., Karssenbergh D., van Dijk A., 2011. Assimilation of observations of radiation level  
649 into an atmospheric transport model: a case study with the particle filter and the ETEX tracer  
650 dataset. *Atmos. Environ.*, 6149-6157. <https://doi.org/10.1016/j.atmosenv.2011.08.024>
- 651 Jaferník H., 2019. The Safety of Unmanned Aerial Vehicle (UAV) Missions in Storm and  
652 Precipitation Areas. *SFT* 54(2), 194–204, <https://doi.org/10.12845/sft.53.2.2019.15>
- 653 James M., 2015. Simplified methods of using probit analysis in consequence analysis. *Process*  
654 *Saf. Process.*, 34, 58–63. <https://doi.org/10.1002/prs.11686>
- 655 Jońca, J.; Pawnuk, M.; Bezyk, Y.; Arsen, A.; Sówka, I. 2022. Drone-Assisted Monitoring of  
656 Atmospheric Pollution - A Comprehensive Review. *Sustainability*, 14, 11516.  
657 <https://doi.org/10.3390/su141811516>
- 658 Jones R., Lehr W., Simecek-Beatty D., Reynolds M., 2013. ALOHA® (Areal Locations of  
659 Hazardous Atmospheres) 5.4. 4: Technical Documentation. 2013.
- 660 Kamińska D., Sapiński T., Wiak S., Tikk T., Haamer R., Avots E., Helmi A., Ozcinar C.,  
661 Anbarjafari G., 2019. Virtual Reality and Its Applications in Education: Survey. *Information*,  
662 10(10), 318. doi:10.3390/info10100318.
- 663 Kinaneva D., Hristov G., Raychev J., Zahariev P., 2019. Early Forest Fire Detection Using  
664 Drones and Artificial Intelligence. *Computer Science. 42nd International Convention on*  
665 *Information and Communication Technology, Electronics and Microelectronics (MIPRO)*. 20-  
666 24 May 2019. Opatija · Croatia. Corpus ID: 195883043. DOI:10.23919/MIPRO.2019.8756696
- 667 Lambey V., Prasad A.D., 2021. A review on air quality measurement using an unmanned aerial  
668 vehicle. *Water, Air, & Soil Pollution*, 232(3), 1-32. <https://doi.org/10.1007/s11270-020-04973->  
669 [5](https://doi.org/10.1007/s11270-020-04973-5)

- 670 Lee H.E., Sohn J.R., Byeon S.H., Yoon S.J., Moon K.W., 2018. Alternative risk assessment for  
671 dangerous chemicals in South Korea regulation: Comparing three modeling programs. *Int. J.*  
672 *Environ. Res. Public Health*, 15(8), 1600. <https://doi.org/10.3390/ijerph15081600>
- 673 Liu L., Xu W., Lu X., Zhong B., Guo Y., Lu X., Zhao Y., He W., Wang S., Zhang X., Liu X.,  
674 Vitousek P., 2022. Exploring global changes in agricultural ammonia emissions  
675 and their contribution to nitrogen deposition since 1980. *PNAS Environmental Sciences*  
676 *Sustainability Science*, 119(14), e2121998119. <https://doi.org/10.1073/pnas.2121998119>
- 677 Luo Z., Zhang Y., Chen W., Van Damme M., Coheur P.-F., Clarisse L., 2022. Estimating global  
678 ammonia (NH<sub>3</sub>) emissions based on IASI observations from 2008 to 2018. *Atmos. Chem. Phys.*,  
679 22, 10375–10388. <https://doi.org/10.5194/acp-22-10375-2022>
- 680 Malm W.C., Schichtel B.A., Barna M.G., Gebhart K.A., Rodriguez M.A., Collett Jr. J.L.,  
681 Carrico C.M., Benedict K.B., Prenni A.J., Kreidenweis S.M., 2013. Aerosol species  
682 concentrations and source apportionment of ammonia at Rocky Mountain National Park. *Air*  
683 *Waste Manage. Assoc.*, 63, 1245-63. <http://dx.doi.org/10.1080/10962247.2013.804466>
- 684 Mustapić M., Domitrović A., Radišić T., 2021. Monitoring Traffic Air Pollution Using  
685 Unmanned Aerial Systems. In: Petrović M., Novačko L. (Eds) Transformation of  
686 Transportation. EcoProduction (Environmental Issues in Logistics and Manufacturing).  
687 Springer, Cham. [https://doi.org/10.1007/978-3-030-66464-0\\_11](https://doi.org/10.1007/978-3-030-66464-0_11)
- 688 Nandu V.N., Soman A.R., 2018. Consequence Assessment of Anhydrous Ammonia Release  
689 Using CFD-Probit Analysis. *Process Safety Progress*, 37(4), 525-534.  
690 <https://doi.org/10.1002/prs.11970>
- 691 Naseem S., King A.J., 2018. Ammonia production in poultry houses can affect health of  
692 humans, birds, and the environment -Techniques for its reduction during poultry production.  
693 *Environ. Sci. Pollut. Res.*, 25, 15269–15293. <https://doi.org/10.1007/s11356-018-2018-y>
- 694 National Research Council. 2001. Standing operating procedures for developing acute exposure  
695 guideline levels for hazardous chemicals. Washington, DC: The National Academies Press.  
696 2001. <https://doi.org/10.17226/10122>
- 697 National Research Council. 2010. Acute Exposure Guideline Levels for Selected Airborne  
698 Chemicals: Volume 9. Washington, DC: The National Academies Press.  
699 <https://doi.org/10.17226/12978>
- 700 Neghab M., Mirzaei A., Kargar Shouroki F., Jahangiri M., Zare M., Yousefinejad S., 2018.  
701 Ventilatory disorders associated with occupational inhalation exposure to nitrogen trihydride  
702 (ammonia). *Ind Health.*, 56, 427–435. <https://doi.org/10.2486/indhealth.2018-0014>

- 703 Orozco J.L., Van Caneghem J., Hens L., Gonzalez L., Lugo R., Díaz S., Pedroso I., 2019.  
704 Assessment of an ammonia incident in the industrial area of Matanzas. *Journal of Cleaner*  
705 *Production*, 222, 934-941. <https://doi.org/10.1016/j.jclepro.2019.03.024>
- 706 Pan S.Y., He K.H., Lin K.T., Fan C., Chang C.T., 2022.. Addressing nitrogenous gases from  
707 croplands toward low-emission agriculture. *npj Clim Atmos Sci* 5(1), 43.  
708 <https://doi.org/10.1038/s41612-022-00265-3>
- 709 Pirrone N., Keating T., (Eds), 2010. Hemispheric Transport of Air Pollution 2010. Part B:  
710 Mercury. Air Pollution Studies No. 18. ECONOMIC COMMISSION FOR EUROPE Geneva.  
711 UNITED NATIONS New York and Geneva.
- 712 Pobkrut T., Eamsa-ard T., Kerdcharoen T., 2016. Sensor drone for aerial odor mapping for  
713 agriculture and security services. *13th International Conference on Electrical*  
714 *Engineering/Electronics, Computer, Telecommunications and Information Technology (ECTI-*  
715 *CON)*. 28 June – 1 July 2016. Chiang Mai, Thailand. doi:10.1109/ecticon.2016.7561340
- 716 Rabajczyk A, Zboina J, Zielecka M, Fellner R., 2020. Monitoring of Selected CBRN Threats  
717 in the Air in Industrial Areas with the Use of Unmanned Aerial Vehicles. *Atmosphere*, 11(12),  
718 1373. <https://doi.org/10.3390/atmos11121373>
- 719 Rasheed T., Bilal M., Nabeel F., Adeel M., Iqbal H.M.N., 2019. Environmentally-related  
720 contaminants of high concern: Potential sources and analytical modalities for detection,  
721 quantification, and treatment. *Environment International*, 122, 52-66.  
722 doi:10.1016/j.envint.2018.11.038
- 723 Sapek A., 2013. Ammonia Emissions from Non-Agricultural Sources. *Polish J. Environ. Stud.*  
724 22(1), 63–70. Corpus ID: 98099008
- 725 Šmídl, V., Hofman, R. 2013. Tracking of atmospheric release of pollution using unmanned  
726 aerial vehicles *Atmospheric Environment*, 67, 425-436.  
727 <http://dx.doi.org/10.1016/j.atmosenv.2012.10.054>
- 728 Sommer S.G., Hutchings N.J., Webb J., 2019. New emission factors for calculation of ammonia  
729 volatilization from European livestock manure management systems. *Front. Sustain. Food*  
730 *Syst.*, 3, 101. <https://doi.org/10.3389/fsufs.2019.00101>
- 731 Statistica.com. 2021. Annual ammonia (NH<sub>3</sub>) emissions in the United States from 1990 to 2020.  
732 <https://www.statista.com/statistics/501317/volume-of-ammonia-emissions-us/> (accessed on 20  
733 May 2023)
- 734 Sutton M.A., Dragosits U., Tang Y.S., Fowler D., 2000. Ammonia emissions from non-  
735 agricultural sources in the UK. *Atmos. Environ.*, 34, 855–869. [https://doi.org/10.1016/S1352-](https://doi.org/10.1016/S1352-2310(99)00362-3)  
736 [2310\(99\)00362-3](https://doi.org/10.1016/S1352-2310(99)00362-3)

737 The CAMEO® Software Suite. ALOHA® Example Scenarios. 2016. National Oceanic and  
738 Atmospheric Administration, U.S. Environmental Protection Agency.  
739 [https://response.restoration.noaa.gov/sites/default/files/ALOHA\\_Examples.pdf](https://response.restoration.noaa.gov/sites/default/files/ALOHA_Examples.pdf) (accessed on 1  
740 March 2023)

741 Thykier-Nielsen S., Deme S., Mikkelsen T., 1999. Description of the Atmospheric Dispersion  
742 Module RIMPUFF. Riso National Laboratory. PO Box 49.  
743 <https://citeseerx.ist.psu.edu/document?repid=rep1&type=pdf&doi=f41efa614a5fa79c5a7aafcd>  
744 [ba64a284987b7fe7](https://citeseerx.ist.psu.edu/document?repid=rep1&type=pdf&doi=f41efa614a5fa79c5a7aafcd) (accessed on 17 May 2023)

745 Tseng J.M., Sua T.S., Kuo C.Y., 2012. Consequence evaluation of toxic chemical releases by  
746 ALOHA. *Procedia Engineering*, 45, 384 – 389. <https://doi.org/10.1016/j.proeng.2012.08.175>

747 U.S. Department of Energy, National Nuclear Security Administration, 2007. ATMOSPHERIC  
748 DISPERSION MODEL VALIDATION IN LOW WIND CONDITIONS. FINAL REPORT.  
749 DOE/NV/25946--277

750 U.S. Department of Energy, Office of Environment, Safety and Health, 2004, ALOHA  
751 Computer Code. Application Guidance for Documented Safety Analysis. Final Report. DOE-  
752 EH-4.2.1.3-ALOHA Code Guidance.

753 UNECE. 1999. The 1999 Gothenburg Protocol to Abate Acidification Eutrophication and  
754 Ground-level Ozone. <https://unece.org/gothenburg-protocol> (accessed on 9 June 2023)

755 UNECE. 2019. Amendment of the Text and Annexes II to IX to the Protocol to the 1979  
756 Convention on Long-range Transboundary Air Pollution to Abate Acidification, Eutrophication  
757 and Ground-Level Ozone and the Addition of New Annexes X and XI  
758 C.N.155.2013.TREATIES-XXVII-1-h of 28 February 2013 (Adoption of Amendments to  
759 Annexes II to IX to the Protocol and addition of annexes X and XI).  
760 <https://treaties.un.org/doc/Publication/CN/2013/CN.155.2013-Eng.pdf> (accessed on 17 May  
761 2021).

762 Van Damme M., Clarisse L., Whitburn S., Juliette Hadji-Lazaro J., Hurtmans D., Cathy  
763 Clerbaux C., Coheur P.F., 2018. Industrial and agricultural ammonia point sources exposed.  
764 *Nature* 564, 99–103. <https://doi.org/10.1038/s41586-018-0747-1>

765 Van Damme M.L., Franco B., Sutton M.A., Erisman J.W., Kruit R.W., van Zanten M.,  
766 Whitburn S., Hadji-Lazaro J., Hurtmans D., Cathy Clerbaux C., Coheur P.F., 2021. Global,  
767 regional and national trends of atmospheric ammonia derived from a decadal (2008-2018)  
768 satellite record. *Environ. Res. Lett.*, 16(5), 055017. <https://doi.org/10.1088/1748-9326/abd5e0>

- 769 Vidi N., 2019. Drones and Robots Helped Save Notre Dame. (In) DroneBelow.com,  
770 <https://dronebelow.com/2019/04/19/drones-and-robots-helped-save-notre-dame/> (accessed on  
771 17 May 2023)
- 772 Wu C., Wang G., Li J., Li J., Cao C., Ge S., Xie Y., Chen J., Liu S., Du W., Zhao Z., Cao F.,  
773 2020. Non-agricultural sources dominate the atmospheric NH<sub>3</sub> in Xi'an, a megacity in the semi-  
774 arid region of China. *Sci. Total Environ.*, 722, 137756.  
775 <https://doi.org/10.1016/j.scitotenv.2020.137756>
- 776 Wu Y., Gu B., Erismann J.W., Reis S., Fang Y., Lu X., Zhang X., 2016. PM<sub>2.5</sub> pollution is  
777 substantially affected by ammonia emissions in China. *Environ. Pollut.*, 218, 86–94.  
778 doi:10.1016/j.envpol.2016.08.027
- 779 Wyer K.E., Kelleghan D.B., Blanes-Vidal V., Schauburger G., Curran T.P., 2022. Ammonia  
780 emissions from agriculture and their contribution to fine particulate matter: A review of  
781 implications for human health. *Journal of Environmental Management*, 323, 116285.  
782 <https://doi.org/10.1016/j.jenvman.2022.116285>
- 783 Xiang T.-Z., Xia G.-S., Zhang L., 2019. Mini-Unmanned Aerial Vehicle-Based Remote  
784 Sensing: Techniques, applications, and prospects. *IEEE Geoscience and Remote Sensing*  
785 *Magazine*, 7(3), 29–63. doi:10.1109/mgrs.2019.2918840
- 786 Zappa C.J., Brown S.M., Laxague N.J.M., Dhakal T., Harris R.A., Farber A.M., Subramaniam  
787 A., 2020. Using Ship-Deployed High-Endurance Unmanned Aerial Vehicles for the Study of  
788 Ocean Surface and Atmospheric Boundary Layer Processes. *Front. Mar. Sci.*, 6, 777. doi:  
789 10.3389/fmars.2019.00777
- 790 Zhan X., Adalibieke W., Cui X., Winiwarter W., Reis S., Zhang L., Bai Z., Wang Q., Huang  
791 W., Zhou F., 2021. Improved Estimates of Ammonia Emissions from Global Croplands.  
792 *Environ. Sci. Technol.*, 55, 2, 1329–1338. <https://doi.org/10.1021/acs.est.0c05149>
- 793 Zheng J., Ma Y., Chen M., Zhang Q., Wang L., Alexei F., Khalizov A.V., Yao L., Wang Z.,  
794 Wang X., Chen L., 2015. Measurement of atmospheric amines and ammonia using the high  
795 resolution time-of-flight chemical ionization mass spectrometry. *Atmos. Environ.*, 102, 249-  
796 259. <http://dx.doi.org/10.1016/j.atmosenv.2014.12.002>